Science Advances
AAAS

Supplementary Materials for

DDM1-mediated R-loop resolution and H2A.Z exclusion facilitates heterochromatin formation in Arabidopsis

Jincong Zhou *et al.*

Corresponding author: Qianwen Sun, sunqianwen@mail.tsinghua.edu.cn

Sci. Adv. **9**, eadg2699 (2023)
DOI: 10.1126/sciadv.adg2699

The PDF file includes:

Figs S1 to S19
Legends for data S1 to S7

Other Supplementary Material for this manuscript includes the following:

Data S1 to S7

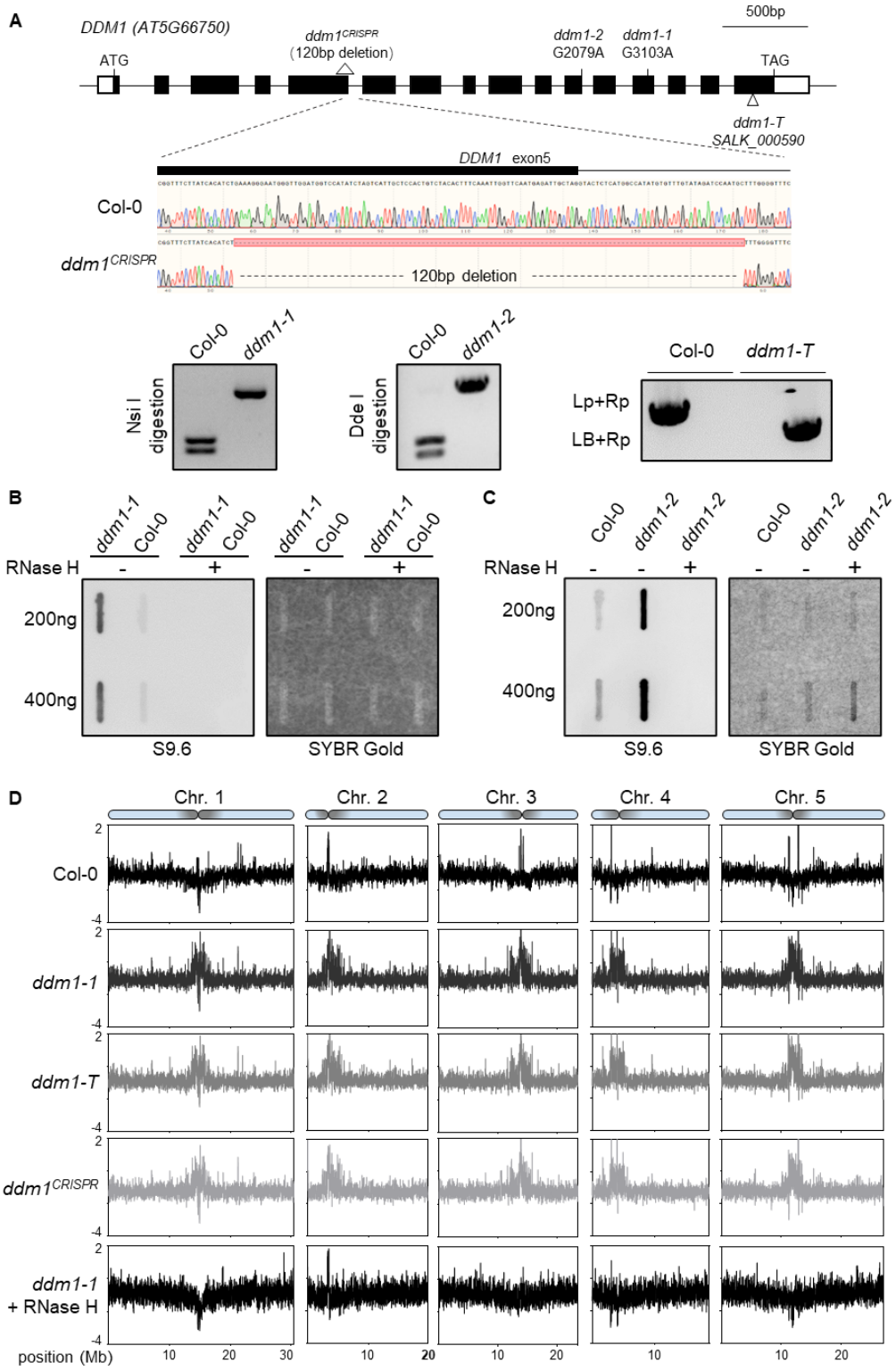

fig. S1. DDM1 is a major restrictor for pericentromeric R-loop homeostasis. (A) Genotypes of *ddm1* mutants. Sequencing chromatograms show the deletion of the *DDM1* loci in CRISPR/Cas9-based genomic DNA deletion mutant. PCR results show the genotypes of *DDM1* in *ddm1-1*, *ddm1-2* and *ddm1-T* (*SALK_000590*). **(B and C)** Slot-blots show R-loop levels detected by S9.6 antibody in WT and *ddm1-1* and *ddm1-2.* The membrane was stained with SYBR Gold

as a loading control. **(D)** ssDRIP-seq data of different allelic mutants of *ddm1.* Log_2(S9.6-IP/input) values are plotted in 10-kb bins on chromosomes.

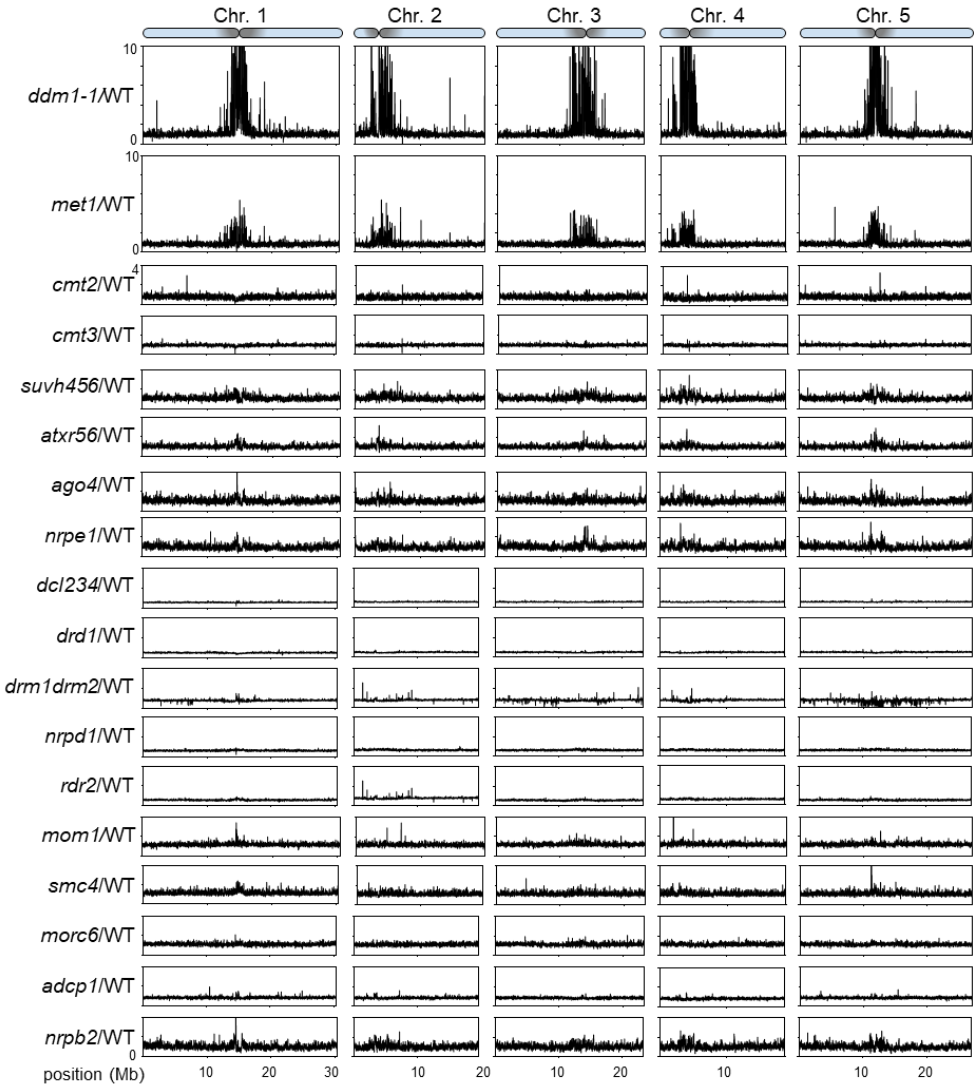

fig. S2. R-loop levels of mutants involved in pericentromeric heterochromatin formation in Arabidopsis. ssDRIP-seq based screen of mutants involved in heterochromatin formation in Arabidopsis. Mutant/WT values from ssDRIP-seq are plotted in 10-kb bins on chromosomes as shown in Fig. 1A. Information of mutants was listed in data S1.

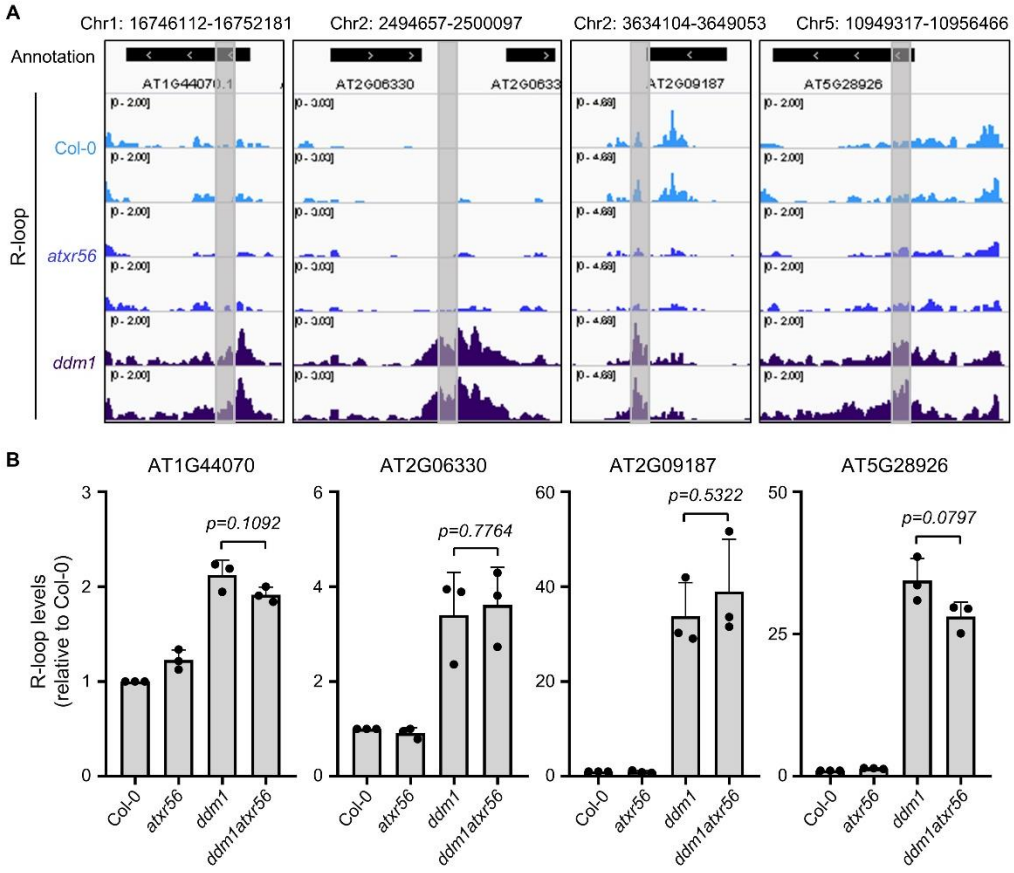

fig. S3. DDM1 is epistasis to the ATXR5/ATXR6 on R-loop clearance. (A) Snapshots of Integrative Genomics Viewer showing R-loops in Col-0, *atxr5atxr6*, *ddm1* on DRIP-qPCR tested loci. Gray boxes indicate the tested regions by DRIP-qPCR. **(B)** DRIP-qPCR shows relative R-loop levels in Col-0, *atxr5atxr6*, *ddm1*, *ddm1atxr5atxr6* on tested loci. Mean + SD with three replicates.

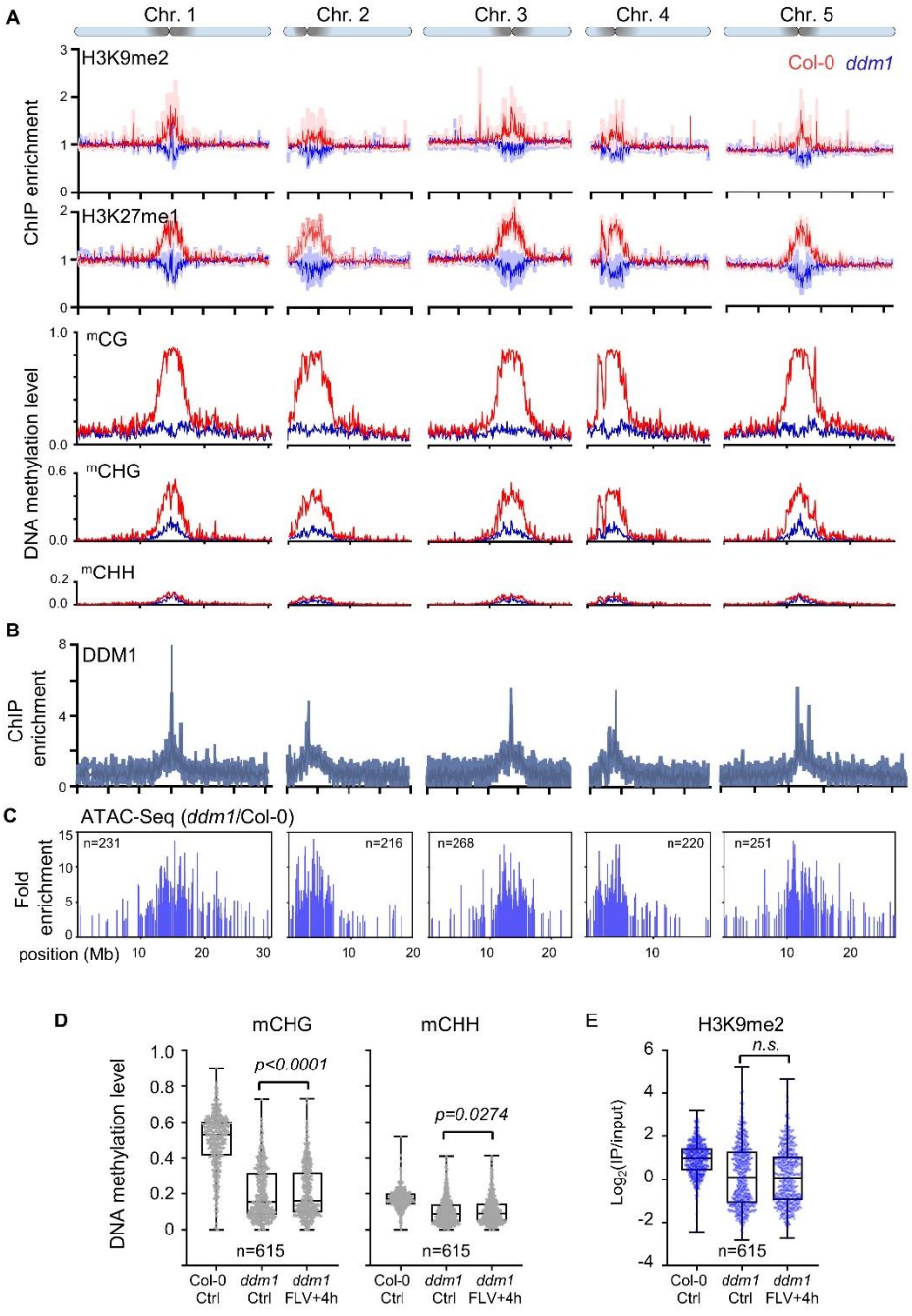
A
Chr. 1
Chr. 2
Chr. 3
Chr. 4
Chr. 5
H3K9me2
Col-0 ddm1
ChIP enrichment
H3K27me1
DNA methylation level
mCG
mCHG
mCHH
B
DDM1
ChIP enrichment
C
ATAC-Seq (ddm1/Col-0)
Fold enrichment
n=231
n=216
n=268
n=220
n=251
position (Mb)
D
mCHG
mCHH
DNA methylation level
p<0.0001
p=0.0274
n=615
Col-0 Ctrl
ddm1 Ctrl
ddm1 FLV+4h
E
H3K9me2
n.s.
Log2(IP/input)
n=615
Col-0 Ctrl
ddm1 Ctrl
ddm1 FLV+4h

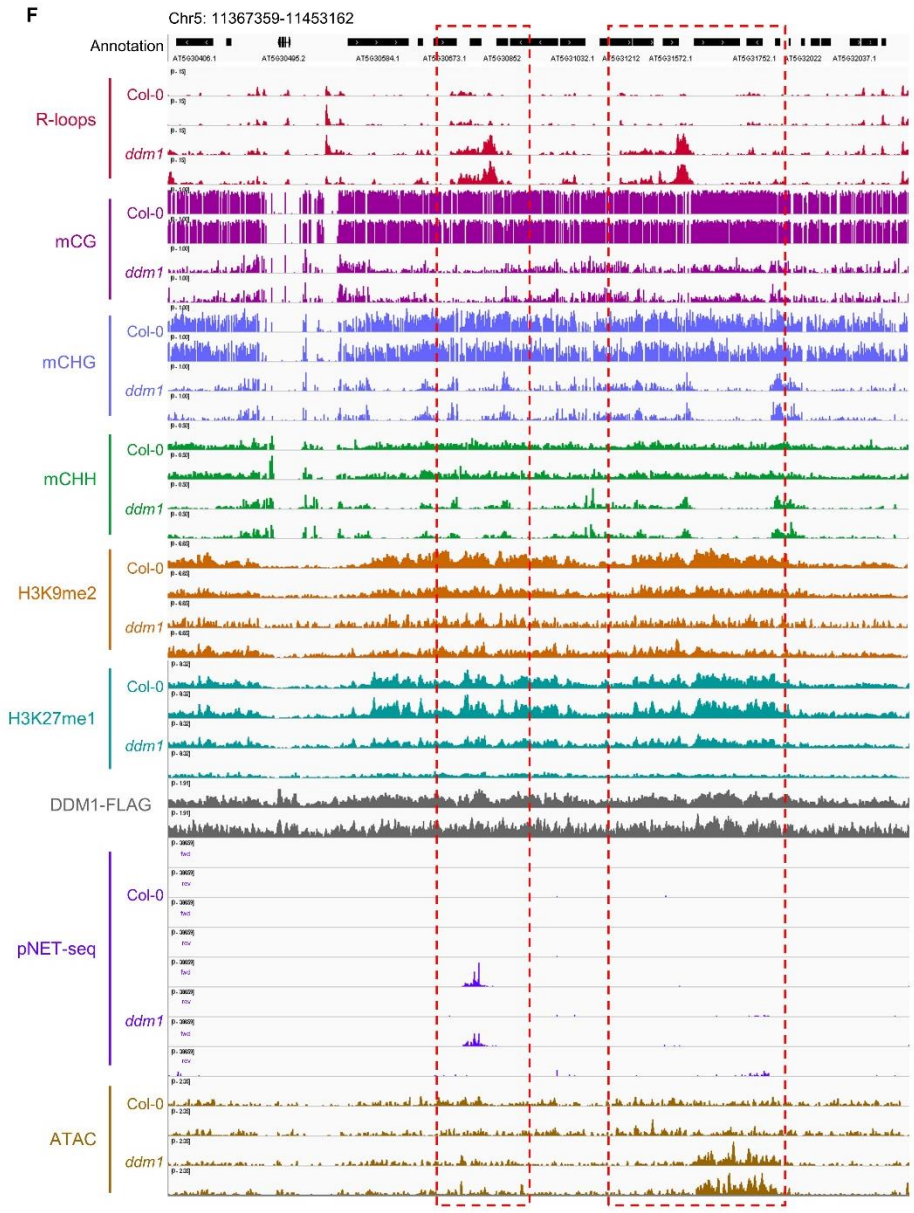

fig. S4. Co-transcriptional R-loops accumulation disturbs pericentromeric heterochromatin formation in *ddm1* mutant. (A) H3K9me2 ChIP-seq (normalized to H3), H3K27me1 ChIP-seq (normalized to H3) and DNA methylation levels in Col-0 and *ddm1* from two biological replicates plotted for the five chromosomes. **(B)** DDM1-FLAG ChIP-seq enrichment scores on chromosomes. Positive values of IP(DDM1-FLAG)-IP(Col-0) from two biological replicates were used for calculating DDM1 enrichment scores. **(C)** Peaks with significant enriched ATAC-seq signal (RPKM) in ddm1 vs Col-0 on chromosomes. n is for the number of peaks on each chromosome. **(D)** Box and Whisker plot showing CHG and CHH DNA methylation levels after 4h flavopiridol treatment. Min to max and interquartile range are shown. **(E)** Box and Whisker plot showing H3K9me2 levels after 4h flavopiridol treatment. Min to max and interquartile range are shown. **(F)** Snapshots of Integrative Genomics Viewer showing R-loop, DNA methylation (CG, CHG and CHH), H3K9me2, H3K27me1, DDM1-FLAG ChIP, pNET-seq and ATAC-seq in Col-0 and *ddm1.* Two replicates are shown.

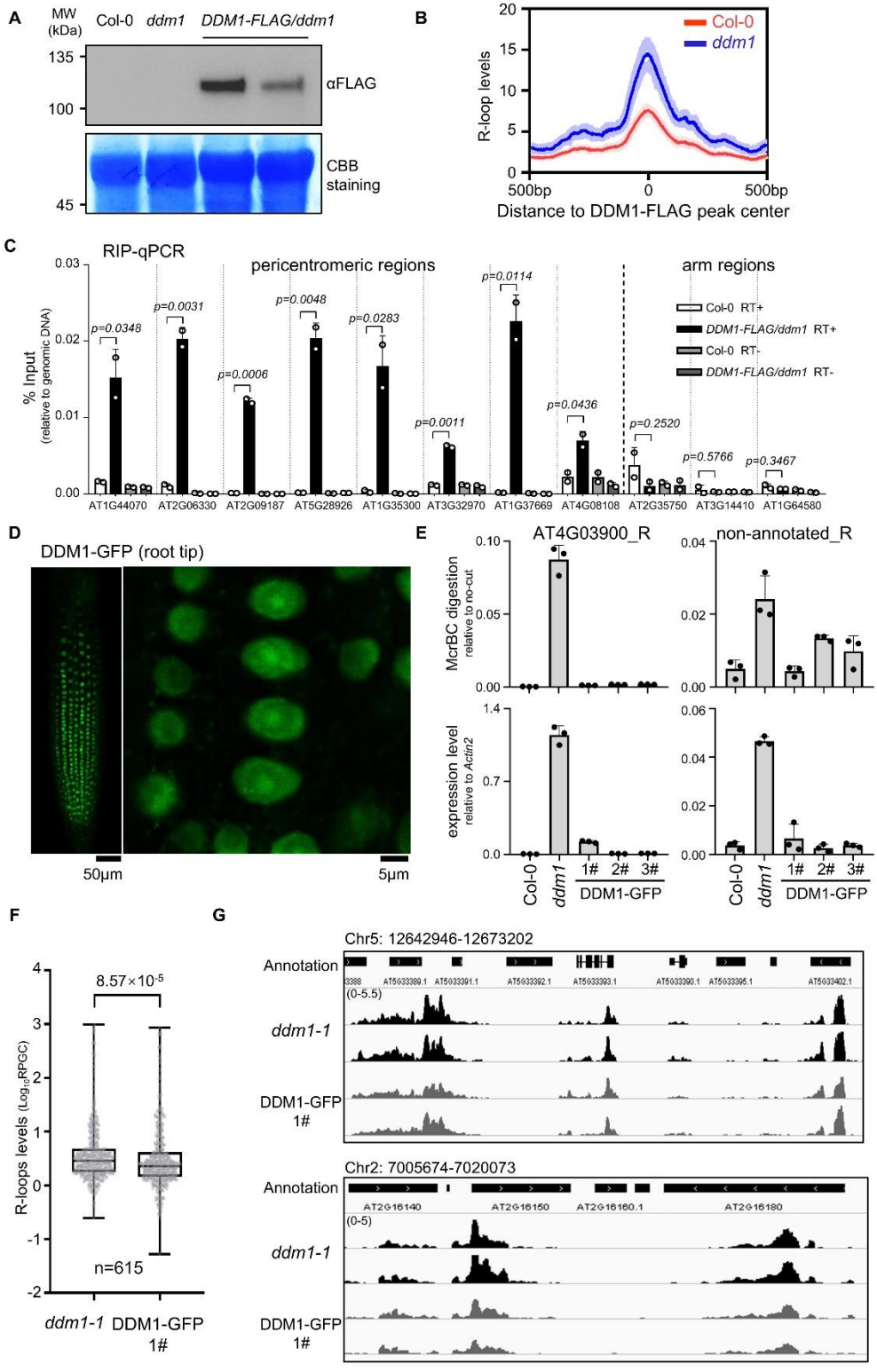

fig. S5. Validation DDM1 complementation lines. (A) Western blot analysis of DDM1-FLAG complementation lines using the FLAG antibody. **(B)** R-loop levels (RPGC) around the DDM1 FLAG ChIP-seq peak center in Col-0 and *ddm1*. The solid lines represent the average, while the faded lines represent the two biological replicates. **(C)** RIP-qPCR analysis to show the DDM1 binding to RNAs from different chromosome loci. Pericentromeric loci (on the left, n=8)

showed the accumulated R-loops in the *ddm1* mutant (according to the ssDRIP-seq data from Fig.1). Chromosome arm-located loci (on the right, n=3) showed no difference in R-loop levels between WT and *ddm1.* Col-0 samples (Col-0 RT+) and minus RT samples (RT-) are used as negative controls. Mean + SD with two replicates. **(D)** GFP signal in the root tip of DDM1-GFP complementation plants. **(E)** Chop-qPCR and RT-qPCR showing DNA methylation levels and transcription levels of two selected TEs in WT, *ddm1* and three independent DDM1-GFP complementation lines. Mean + SD with three replicates. **(F)** Scatter dot plot showing R-loops levels (Log_{10}RPGC) of *ddm1-1* and DDM1-GFP complementation line 1 on increased R-loop peaks in *ddm1* (n=615). Min to max and interquartile range are shown. **(G)** Snapshots of Integrative Genomics Viewer showing R-loop in *ddm1-1* and DDM1-GFP complementation line 1.

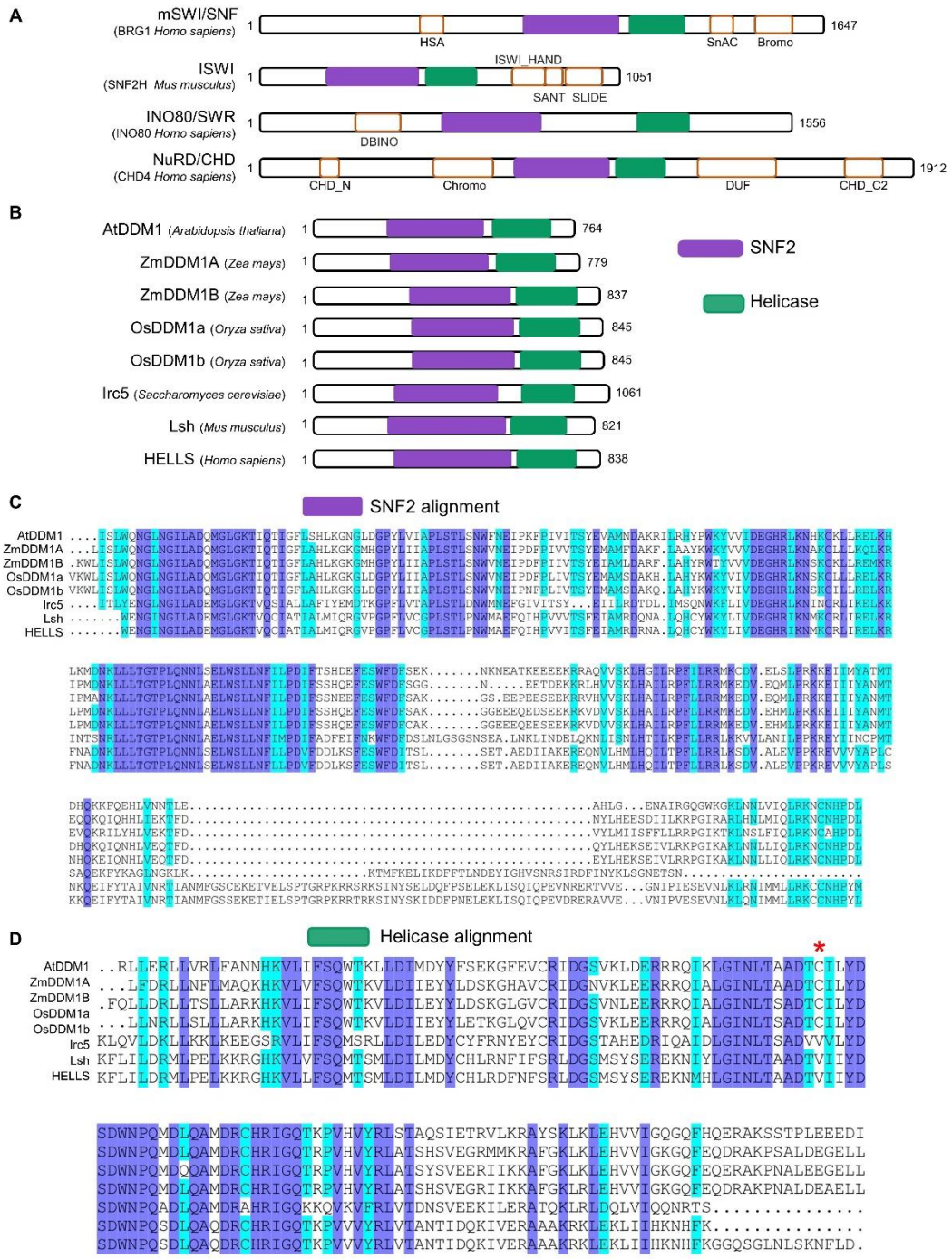

fig. S6. DDM1 orthologs in different species. (A) Schematic architecture of chromatin remodeler subfamilies. SNF2 and helicase domains are shown as purple and green boxes, respectively. **(B)** Schematic architecture of DDM1 orthologs in different species. **(C)** Alignment of amino acid sequences of the SNF2 domain in DDM1 orthologs. **(D)** Alignment of amino acid sequences of the helicase domain in DDM1 orthologs. The asterisk indicates the mutation site in the *ddm1-1* mutant, which is conserved within plants.

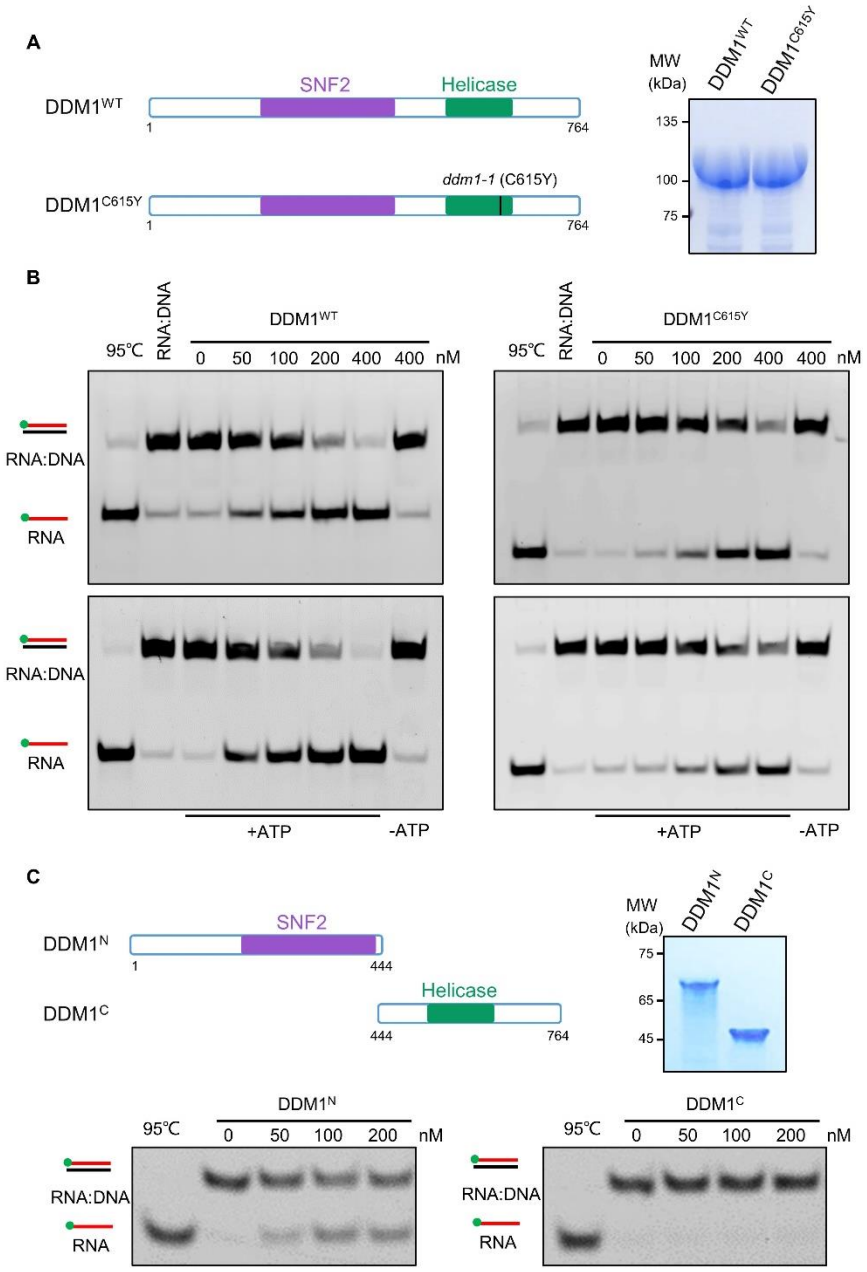

fig. S7. DDM1 resolves RNA:DNA hybrids in vitro. (A) Left, schematic architecture of wild-type and mutant DDM1 proteins. Right, coomassie staining showing the purified recombinant His-tagged wild-type and mutant DDM1, which is used in helicase activity assays (in Fig. 3C). **(B)** Two replicates of helicase activity assays using wild-type and mutant DDM1 proteins under the substrate of RNA:DNA hybrids. **(C)** Top, schematic architecture, Coomassie and staining picture of the purified recombinant His-tagged DDM1 fragments $DDM1^{N}$ and $DDM1^{C}$. Bottom, helicase activity assays using $DDM1^{N}$ and $DDM1^{C}$ under the substrate of RNA:DNA hybrids.

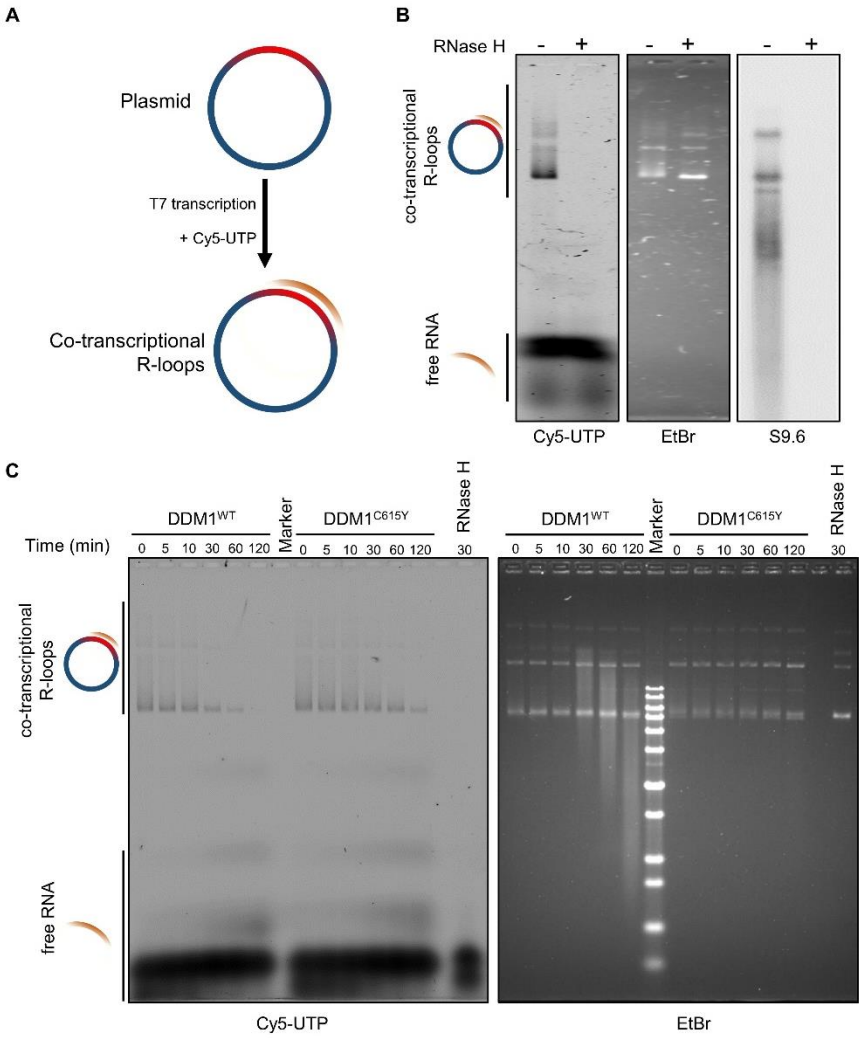

fig. S8. DDM1 resolves R-loops in vitro. (A) Schematic representation showing how co-transcriptional R-loops are generated. 5 µg of plasmid is in vitro transcribed by adding Cy5 fluorescence labeled UTP. Co-transcriptional R-loop substrates were purified for R-loop resolving assays (see Methods). **(B)** Validation of co-transcriptional R-loops. Left, R-loop products with or without RNase H treatment are detected by Typhoon FLA9500 using a Cy5 filter. Middle, gel is stained with EtBr to indicate the loading amount. Right, nuclei acids on the gel are slotted onto a nitrocellulose Hybond N+ membrane then detected by RNA:DNA antibody S9.6. **(C)** Left, R-loop substrates were incubated with indicated proteins (3 µM) for 0, 10, 30, 60 or 120 min then detected by Cy5 signal on gels (see Methods). Right, loading amounts are shown on the EtBr-stained gels.

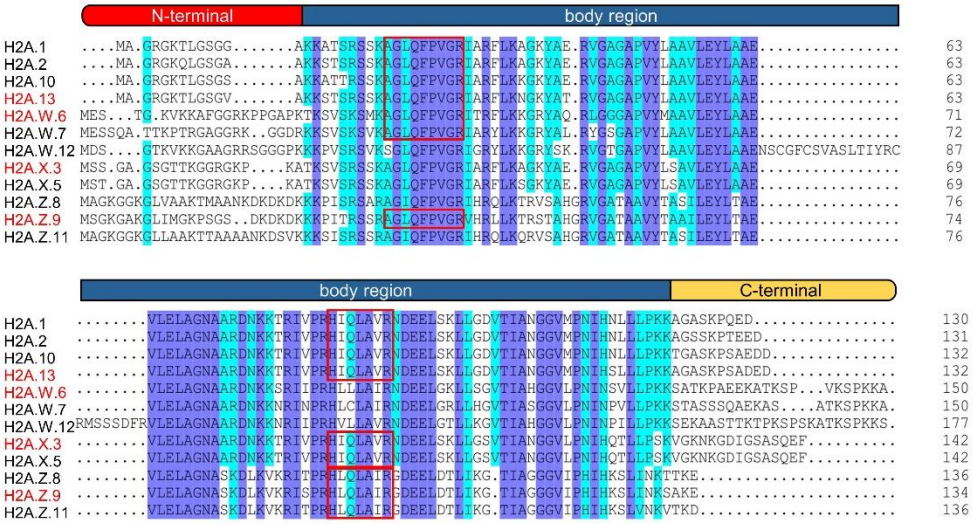

fig. S9. Arabidopsis histone 2A variants. Alignments of amino acid sequences of Arabidopsis histone 2A variants. Red boxes indicate identified peptides in DDM1-GFP IP-MassSpec assays (data S2-S5).

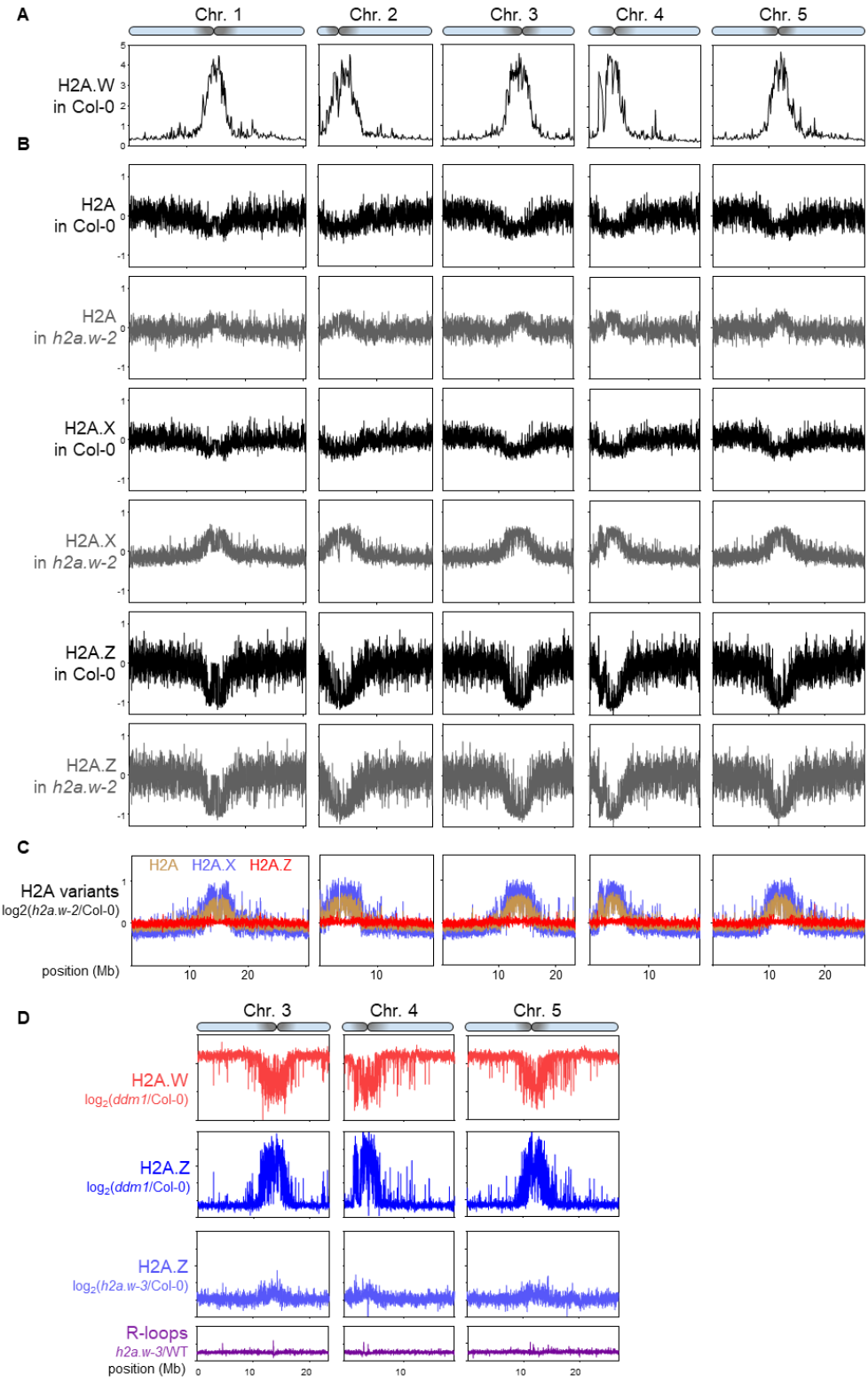

fig. S10. H2A and H2A.X replace H2A.W in the absence of H2A.W. (A) H2A.W ChIP-seq [$\log_2$(IP/input)] are plotted on chromosomes. Data are from published data (*45*). **(B)** ChIP-seq data of H2A, H2A.X and H2A.Z [$\log_2$(IP/input)] from

WT and *h2a.w-2* are plotted on chromosomes. Data are from published data (*15*). **(C)** Abundance of H2A variants changes in *h2a.w* relative to WT. Data are from published data (*15*). **(D)** Continued with related Fig. 4C.

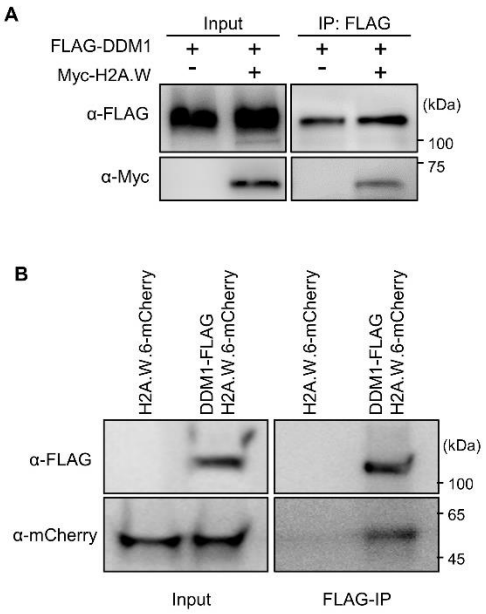

fig. S11. DDM1 interacts with H2A.W. (A) Co-immunoprecipitation followed by western blot analysis showing interaction between DDM1 and H2A.W. FLAG-DDM1 and Myc-H2A.W.6-GFP were transiently expressed in Arabidopsis protoplast and immunoprecipitated by FLAG beads. **(B)** Co-immunoprecipitation followed by western blot analysis showing interactions between DDM1 and H2A.W with native promoter-drived transgene plants.

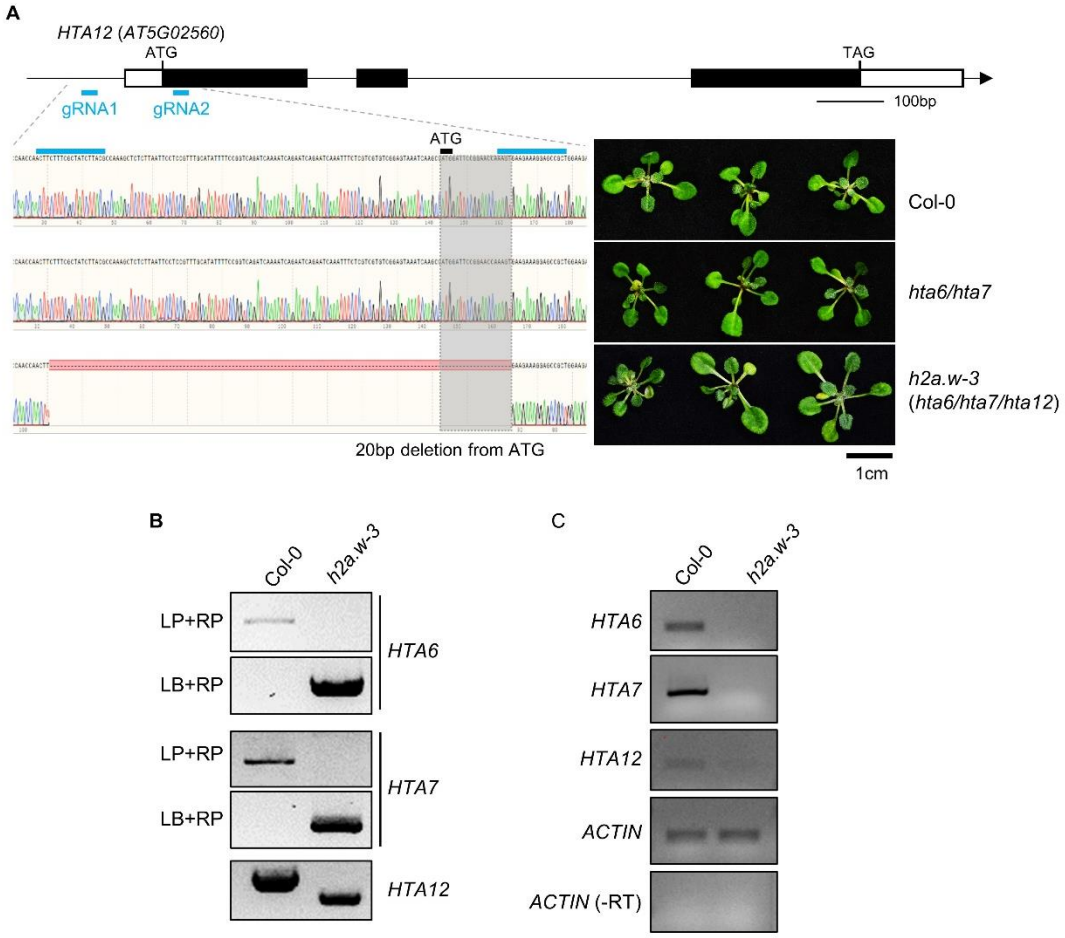

fig. S12. Generation of *h2a.w-3* triple mutant by CRISPR-Cas9. (A) Sequencing chromatograms showing deletion of the *HTA12* loci in *hta6/hta7* to generate the *h2a.w-3* (*hta6/hta7/hta12*) mutant. Blue lines denote CRISPR guide RNA positions. There is a 20 bp deletion from ATG on the *HTA12* coding region. Scale bar, 1 cm. **(B)** PCR results showing genotypes of *HTA6, HTA7* and *HTA12* in WT and *h2a.w-3.* **(C)** RT-PCR results showing expression levels of *HTA6, HTA7* and *HTA12* in WT and *h2aw-3*. *ACTIN* and *ACTIN* (-RT) were used as the control.

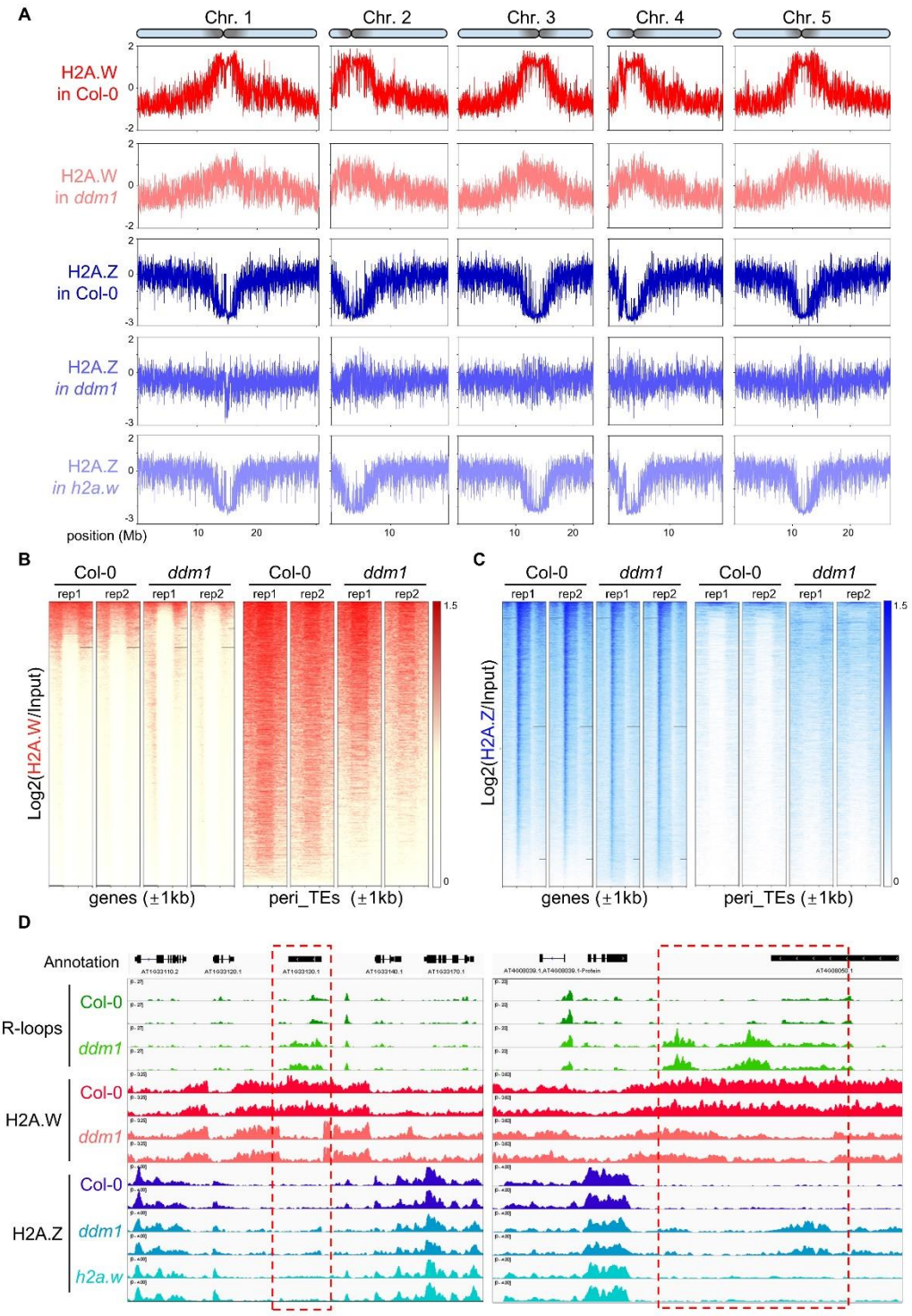
A
Chr. 1
Chr. 2
Chr. 3
Chr. 4
Chr. 5
H2A.W in Col-0
H2A.W in ddm1
H2A.Z in Col-0
H2A.Z in ddm1
H2A.Z in h2a.w
position (Mb)
B
Col-0
ddm1
rep1
rep2
Log2(H2A.W/Input)
genes (±1kb)
peri_TEs (±1kb)
C
Log2(H2A.Z/Input)
D
Annotation
R-loops
H2A.W
H2A.Z
h2a.w

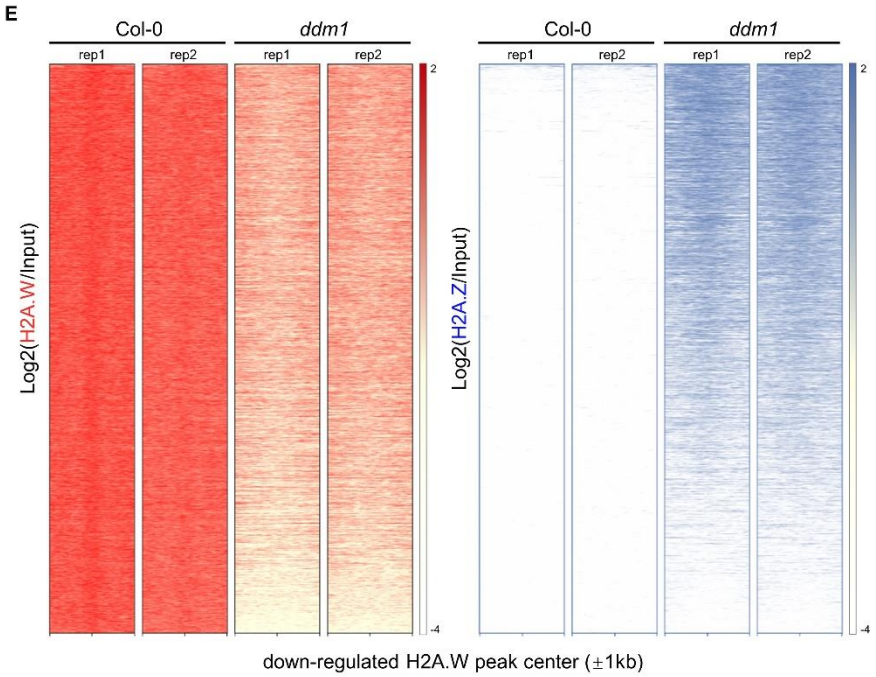

fig. S13. The depositions of pericentromeric H2A.W and H2A.Z are affected in the *ddm1* mutant. (A) H2A.W.6-FLAG ChIP-seq results in WT and *ddm1*, and H2A.Z ChIP-seq results in Col-0, *ddm1*, and *h2a.wa*re plotted in 10-kb bins on the five chromosomes. IP normalized to input values from two replicates are presented. **(B and C)** Heat maps showing the enrichment of H2A.W.6-FLAG and H2A.Z over annotated total genes (n=33,323) and pericentromeric TEs (n=17,598) in WT and *ddm1.* Color bar scale indicates $\log_2$(IP/input). **(D)** Snapshots of Integrative Genomics Viewer showing R-loop, H2A.W.6-FLAG and H2A.Z in the indicated samples. Two replicates for each sample are shown. **(E)** Heatmaps showing H2A.W and H2A.Z levels are plotted at H2A.W peaks downregulated in *ddm1.* All values are presented by sorting down-regulated H2A.W peaks (n=4,793).

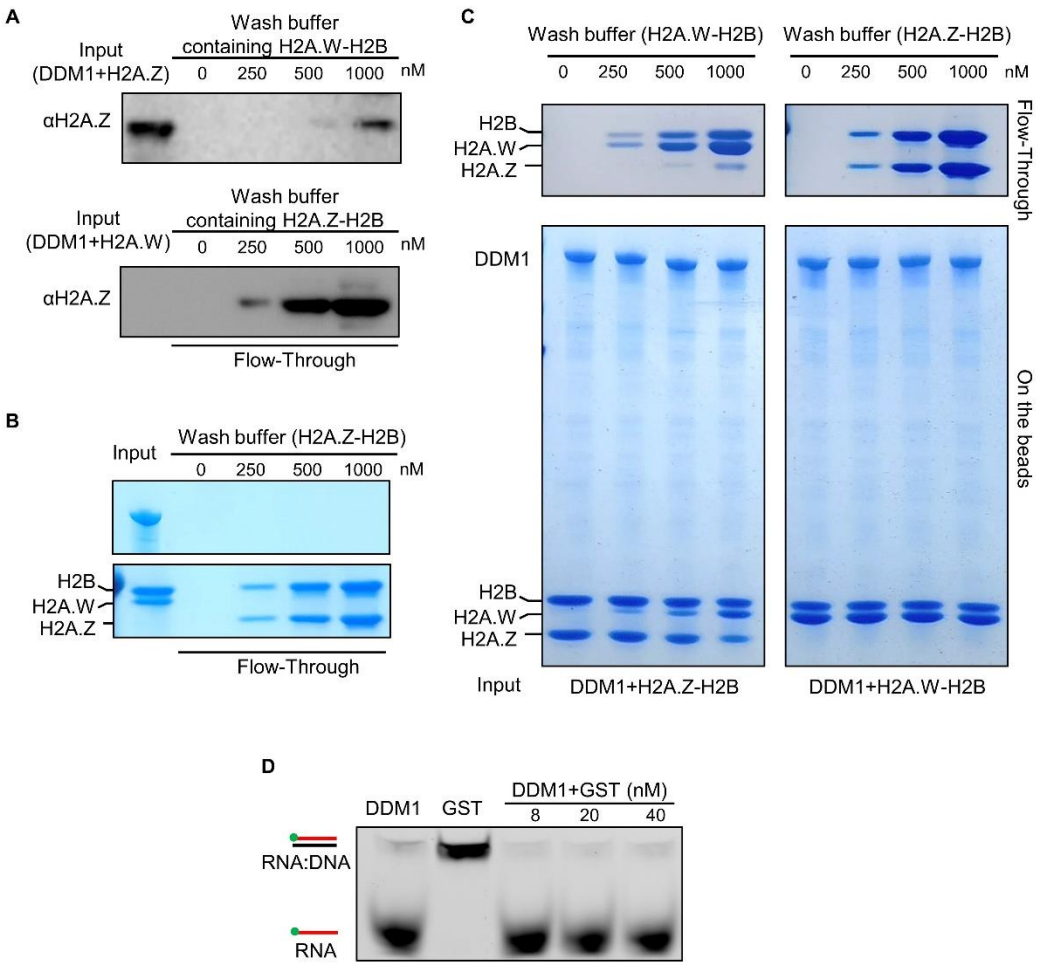

fig. S14. H2A.W disrupts DDM1-H2A.Z interaction. (A) Top, competitive pull-down experiment was conducted as same as Fig. 4C left, except the native anti-H2A.Z antibody was used in Western blotting. Bottom, relative to fig. S14B, the native anti-H2A.Z antibody was used in Western blotting. **(B)** Related to Fig. 4E, wash buffer containing H2A.Z was used to dissociate DDM1-H2A.W complexes. **(C)** Related to Fig. 4E and S14B, the proteins both in wash buffer and on beads are shown via PAGE gel staining. **(D)** RNA:DNA helicase activities of DDM1 were not affected by adding control protein GST.

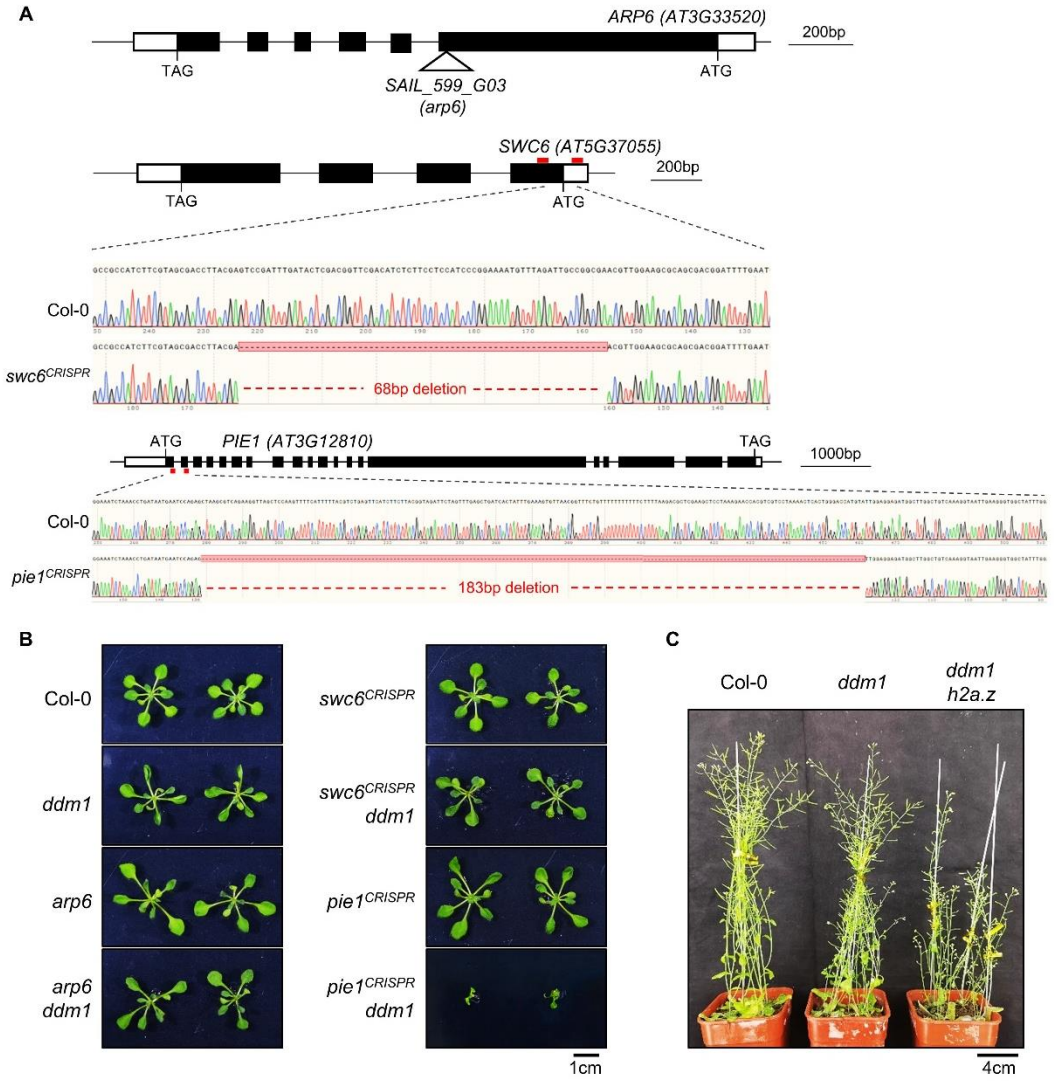

fig. S15. Generation of *swr ddm1 double* mutants. (A) Schematic representation showing the *arp6* mutants used to generate *arp6ddm1* double mutants. Sequencing chromatograms showing deletion of the *SWC6* and *PIE1* genes. **(B)** 14-day-old seedlings of indicated genotype plants. **(C)** Phenotypes of Col-0, *ddm1* and *ddm1h2a.z* seedlings in soil.

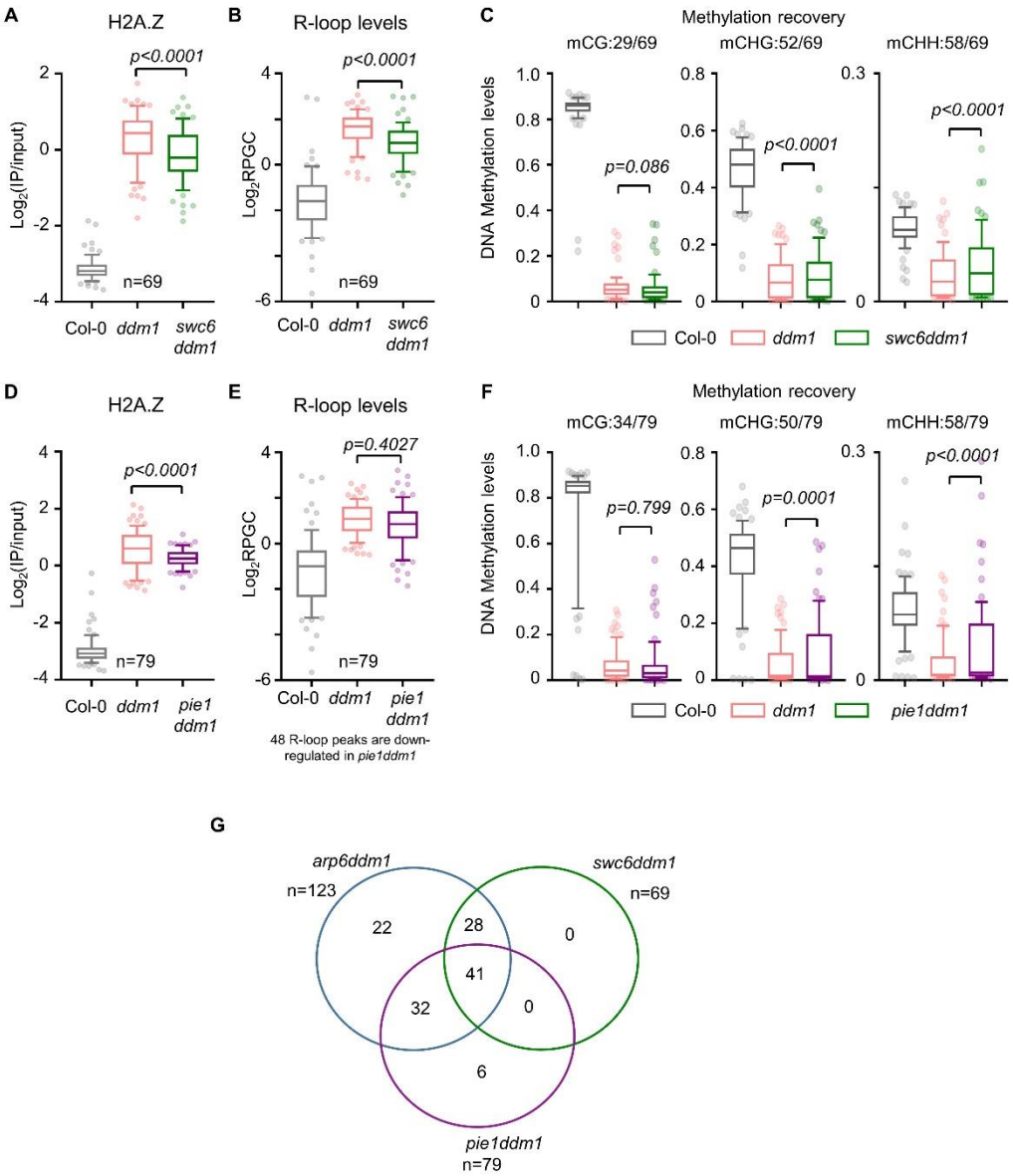

fig. S16. Suppression of H2A.Z deposition in pericentromeric regions rescues the R-loops and DNA methylation defects in *ddm1* mutant. (A) 69 up-regulated pericentromeric R-loop peaks of *ddm1* showed decreased H2A.Z abundance in *swc6ddm1*. **(B)** R-loop levels of 69 decreased H2A.Z peaks in Col-0, *ddm1* and *swc6ddm1*. **(C)** DNA methylation levels of 69 decreased H2A.Z peaks in Col-0, *ddm1* and *swc6ddm1*. **(D)** 79 up-regulated pericentromeric R-loop peaks of *ddm1* showed decreased H2A.Z abundance in *pie1ddm1*. **(E)** R-loop levels of 79 decreased H2A.Z peaks in Col-0, *ddm1* and *pie1ddm1*. **(F)** DNA methylation levels of 79 decreased H2A.Z peaks in Col-0, *ddm1* and *pie1ddm1*. All data above are shown with 10% to 90% and interquartile range. **(G)** Overlaps of up-regulated R-loop peaks in three double mutants (*arp6ddm1*, *swc6ddm1* and *pie1ddm1*).

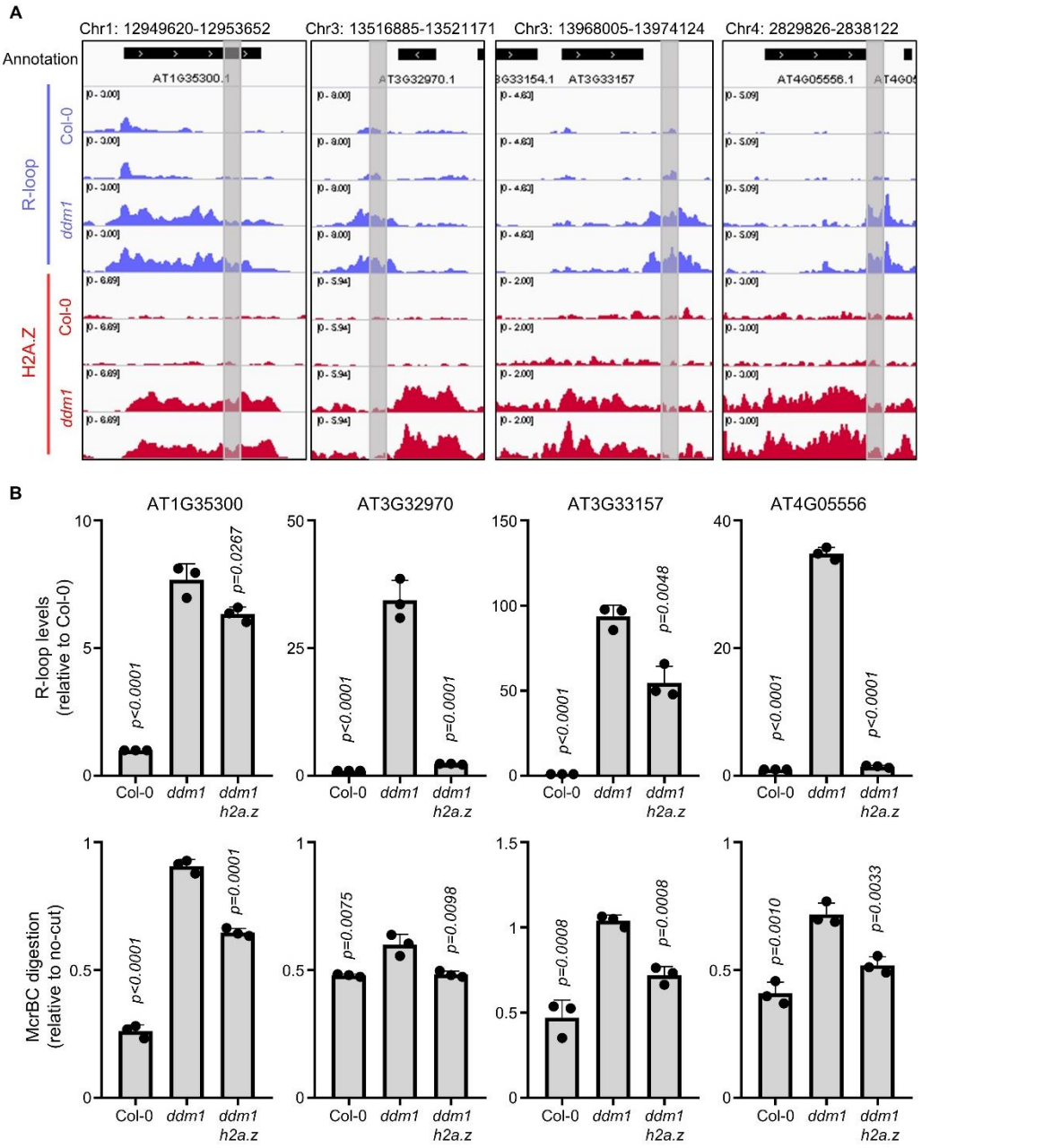

fig. S17. Loss of H2A.Z rescues the R-loops and DNA methylation defects in *ddm1* mutant. (A) Snapshots of Integrative Genomics Viewer showing R-loops and H2A.Z abundance in Col-0 and *ddm1* on qPCR tested loci in fig. S17B. Gray boxes indicate the tested regions by qPCR in fig. S17B. **(B)** DRIP-qPCR and Chop-qPCR showing R-loop and DNA methylation levels of selected loci in Col-0, *ddm1* and *ddm1h2a.z*. Mean + SD with three replicates.

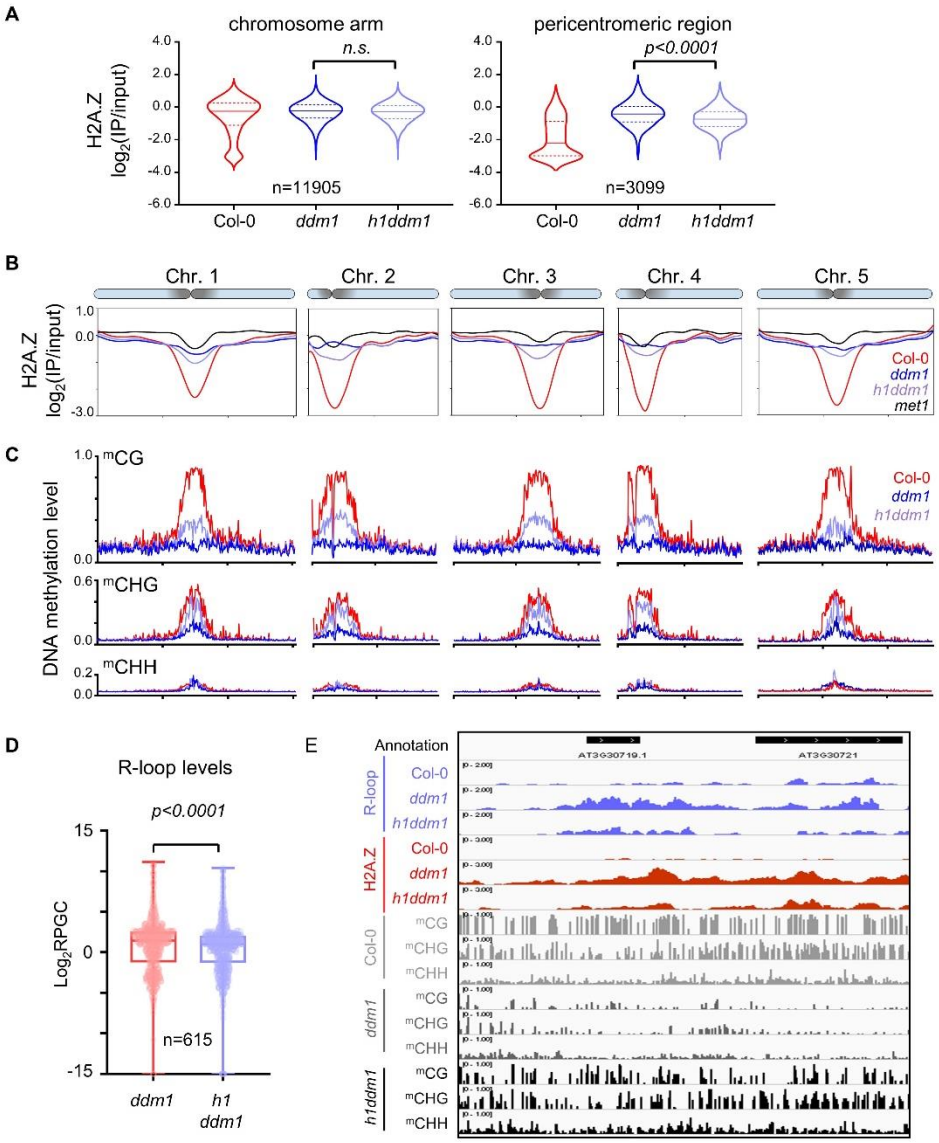

fig. S18. Histone Linker H1 promotes pericentromeric H2A.Z deposition in the *ddm1* mutant. (A) H2A.Z enrichment [log_2(IP/input)] of Col-0, *ddm1*, *h1ddm1* on chromosome arm and pericentromeric region. The genome is divided into windows (100kb/window), and windows are grouped into chromosome arm and pericentromeric region. H2A.Z enrichment [log_2(IP/input)] was calculated on each window and then was plotted. Median and interquartile range are shown. **(B)** H2A.Z ChIP-seq [log_2(IP/input)] are plotted on chromosomes of Col-0, *ddm1, h1ddm1* and *met1.* **(C)** DNA methylation levels in Col-0, *ddm1* and *h1ddm1.* **(D)** R-loop levels that up-regulated in *ddm1* were globally decreased in *h1ddm1.* Min to max and interquartile range are shown. **(E)** Snapshots from Integrative Genomics Viewer showing R-loop, H2A.Z, and DNA methylation levels in WT, *ddm1* and *h1ddm1.*

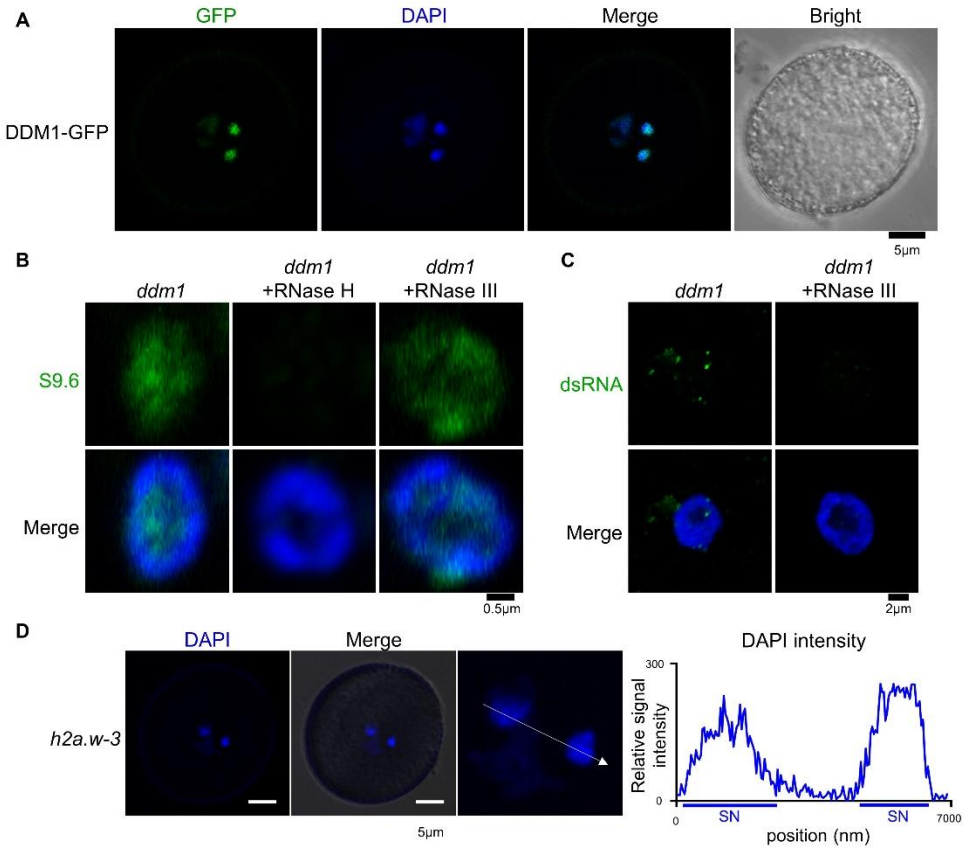

fig. S19. DDM1-facilitated R-loop resolution and H2A.Z eviction is important for tricellular nuclei development in pollen. (A) Microscopic images showing DDM1-GFP in intact pollen. Scale bar, 5μM. **(B)** SN from *ddm1* with or without RNase H/RNase III treatment were immunostained using S9.6 antibodies. Results indicate that dsRNA does not affect S9.6 staining. Scale bar, 0.5 μM. **(C)** Nuclei from *ddm1* with or without RNase III treatment were immunostained using anti-dsRNA antibody. Scale bar, 2μM. **(D)** DAPI staining and relative DAPI intensity of SN from intact pollen of *h2a.w-3*.

Data S1. The detailed information of the mutants used for ssDRIP-seq.

Data S2. Mass spectrometry analysis of GFP immunoprecipitation in DDM1-GFP line #1.

Data S3. Mass spectrometry analysis of GFP immunoprecipitation in DDM1-GFP line #2.

Data S4. Mass spectrometry analysis of GFP immunoprecipitation in DDM1-GFP line #3.

Data S5. Mass spectrometry analysis of GFP immunoprecipitation in mutant *ddm1*.

Data S6. Oligos used for ATPase assays.

Data S7. Primers used in this study.